

## Supplementary Information

### Digital Electrical Impedance Analysis for Single Bacterium Sensing and Antimicrobial Susceptibility Testing

Brian Scherert<sup>†a</sup>, Christine Surette<sup>†a</sup>, Hui Li<sup>b</sup>, Peter Torab<sup>b</sup>, Erik Kvam<sup>a</sup>, Craig Galligan<sup>a</sup>, Steven Go<sup>a</sup>, Greg Grossmann<sup>a</sup>, Tyler Hammond<sup>a</sup>, Tammy Johnson<sup>a</sup>, Richard St-Pierre<sup>a</sup>, John R. Nelson<sup>a</sup>, Radislav Potyrailo<sup>a</sup>, Tejas Khire<sup>a</sup>, Wen Hsieh<sup>c</sup>, Tza-Huei Wang<sup>c</sup>, Pak Kin Wong<sup>b</sup>, Chris M. Puleo<sup>\*a,d</sup>

<sup>a</sup> General Electric Research; Niskayuna, NY, USA. E-mail: chrispuleo@ge.com

<sup>b</sup> The Pennsylvania State University; Department of Biomedical Engineering, State College, PA, USA.

<sup>c</sup> The Pennsylvania State University; Department of Mechanical Engineering, State College, PA, USA

<sup>d</sup> Johns Hopkins University, Department of Mechanical Engineering, Baltimore MD, USA. Johns Hopkins University, Department of Biomedical Engineering, Baltimore MD, USA

<sup>†</sup> These authors contributed equally to this work.

#### Supplementary figures

**Fig. S1** Hand-held multiplexed impedance sensor system. (a) Side view showing a prototype PCB-based nanowell array that is loaded into the DIMM socket (instead of the glass slide based nanowell array). (b-e) Benchmark data showing the impedance measured by the ASIC impedance analyzer on the multiplexed impedance sensor system matched the impedance measured on a bench top impedance analyzer (Keysight E49990A). Panels b and c show impedance data measured on a reference circuit (this data is repeated from Fig. 1 in the main text). Panels d and e show impedance data measured on a nanowell array loaded with broth only.

**Fig. S2:** Impedance spectra measured on the hand-held multiplexed impedance sensor for a (a) nanowell from a control sample (i.e., broth only, no bacteria) and a nanowell that contains *E. coli*.

**Fig. S3** Intrinsic bulk conductivity differences among typical microbial mediums used for AST. Conductivity was measured using a Mettler-Toledo Seven Compact meter that was calibrated against 12.89 mS Standard Conductivity Calibration Solution. Two 1-mL aliquots of medium were sampled and analyzed, with careful washing of the Mettler-Toledo conductivity probe between each measurement. A final measurement against 12.89 mS Calibration Solution is shown to demonstrate effective probe washing. The contents of each growth medium are listed and support a potential relationship between salt content and bulk conductivity.

**Fig. S4** Numerical simulation to estimate the oxygen concentration in the microfluidic device. (a-b) Depletion of oxygen in microfluidic chambers at a bacterial load of (a) 107 and (b) 109 cfu/ml. (c) Schematic of the 2D model of nanoliter chambers for single bacterial growth. Blue arrows indicate oxygen influx from the boundaries (B1-B3). (d) Boundary conditions and parameters of the simulation. B1-B3 have the same oxygen influx. B4 has zero oxygen influx. The numerical calculation was performed in Comsol.

**Fig. S5** Evaporation observed in a nanowell (a) initially at the start of experiment and (b) after 90 minutes. The evaporation rate limits the total experimental duration and needs to be minimized. (c) The impedance from control samples was used to determine the positive detection threshold. For experiments reported in the main text, we used a 3 sigma detection threshold, which classifies a nanowell as positive when the impedance change is less than -31.4%.

**Fig. S6** (a) Kinetic relationship between media conductivity and culture density during AST relative to no-drug control. Experiments were performed with *E. coli* (ATCC 25922) as described in the Materials and Methods for bulk-scale culture conductivity. Culture turbidity was monitored by A600 optical density, after which 1 mL aliquots were clarified by centrifugation and media conductivity was measured on a Mettler-Toledo Seven Compact meter. Significant differences in bulk conductivity and MIC are increasingly observed as the growth of the no-drug control approaches and exceeds OD600 ~1.0 (or ~1 cell/picoliter). After obtaining 1 OD600 (~1 cell/pL), no-drug control measurements are of sufficient dynamic range and persistence to interpret MIC from conductivity data (using either doxycycline or ampicillin). Culture inoculums at Time 0 in these experiments were approximately 0.2 OD600 (or ~2x10<sup>8</sup>/mL) and achieved 1 OD600 (~1 cell/pL) within an hour of culture time, as indicated by the red arrows. (b) Recovery of bulk conductivity in fresh media (after spent media exchange) confirms time-to-detection for achieving ~1 cell/picoliter in no-drug controls. Experiments were performed with *E. coli* as described in the Materials and Methods for bulk-scale culture conductivity. Late log-growth cultures (~1 OD600) were centrifuged and exchanged into fresh media, and conductivity was monitored after media-exchange relative to undisturbed culture controls. The recovery of initial conductivity for cells shifted into fresh media occurs after ~60 minutes of culture time, consistent with Panel A. By extrapolation, this data informs that an hour of culture time should be sufficient for growth detection of *E. coli* in nanoliter culture arrays.

**Fig. S7** (a, b) Comparison of nanoliter culture array data for additional microbial strains using optical monitoring and cell counting. Cultures of *S. epidermidis* (ATCC 35984) and *M. bacteremicum* (ATCC 25791) were loaded into nanoliter culture arrays for optical inspection and digital counting per chamber. Antibiotics were included in duplicate samples to demonstrate AST. (c, d) Recovery of conductivity in fresh media after spent media exchange of (c) *S. epidermidis* (MRSE) or (d) *M. bacteremicum* cultures. Experiments were performed similarly to Fig. S8. The recovery of initial conductivity for MRSE (after exchange into fresh medium) was observed after ~150 minutes of culture time (panel a), whereas for the fastidious *M. bacteremicum* strain (which requires extra medium supplementation with 3% LHB) recovery of conductivity was observed after ~400 minutes of culture time (panel b). By extrapolation, this data informs that much longer culture times (minimum 2.5 hrs) would be required for robust growth detection of these strains in nanoliter culture arrays.

**Fig. S8** The model system from Fig. 3 in the main text was used here to test effect of antimicrobials on bacteria growth. Media conductivity increase is detectably suppressed when bacterial growth is inhibited by antimicrobial drugs. *E. coli* (ATCC 25922) was grown to mid-log phase in rich medium (Tryptic Soy broth) and inoculated into 20 mL fresh medium to a density of 10<sup>8</sup> cells/mL in presence or absence of (a) Kanamycin at 50 µg/mL, or (b) Ampicillin at 40 µg/mL. Each growth condition was replicated in triplicate and measurements made in parallel. Aliquots of 1 mL were withdrawn at indicated times, immediately chilled

on ice, and clarified by centrifugation at 12,000 x g for 5 min at 5°C. The cell-free media supernatant was then flash-frozen at -80°C. Conductivity of the media samples was then measured on a Mettler-Toledo Seven Compact meter.

**Fig. S9** An estimation of the percent coverage of the interdigitated electrode pair during growth and doubling of a single bacterium within a nanowell. Assumptions: one *E. coli* = 2  $\mu\text{m}^2$ , and the surface area of each electrode pair = 40,000  $\mu\text{m}^2$ ). During the two hours of culture reported herein, the maximal electrode coverage by bacteria does not surpass 0.1% of the electrode surface area, which is below the cell and/or particle coverage needed to contribute to impedance-based detection schemes<sup>1-4</sup>. Taken together with Fig. 2, Fig. 6b, and Fig. S10, this suggests the accumulation of metabolites is likely the primary mechanism determining the impedance in the nanowell during growth (and not the physical presence of bacteria on the electrodes).

**Fig. S10** Resistance measured when serial dilutions of conductivity standards ranging from 12.2 to 13.4 mS/cm were loaded directly into the nanowell/sensor chambers (this range of conductivities is consistent with the range of conductivities determined in Fig. 2 to be associated with metabolite specific changes in the growth broth, after centrifuging out any bacteria). The change in resistance associated with the increase in conductivity of the solution within each electrode chamber is consistent with that associated with single bacterium growth.

**Fig. S11** Example data showing comparison of impedance data in a gold (10  $\mu\text{m}$  electrode spacing) and platinum (10  $\mu\text{m}$  electrode spacing) interdigitated electrode sensor. Three sets of nanowells were filled with either growth broth alone before bacteria growth (i.e. LB media; lysogeny broth), broth after 2 hours of bacterial growth (w/ cells), or broth after 2 hours of bacterial growth after removal of cells via centrifugation (w/o cells).

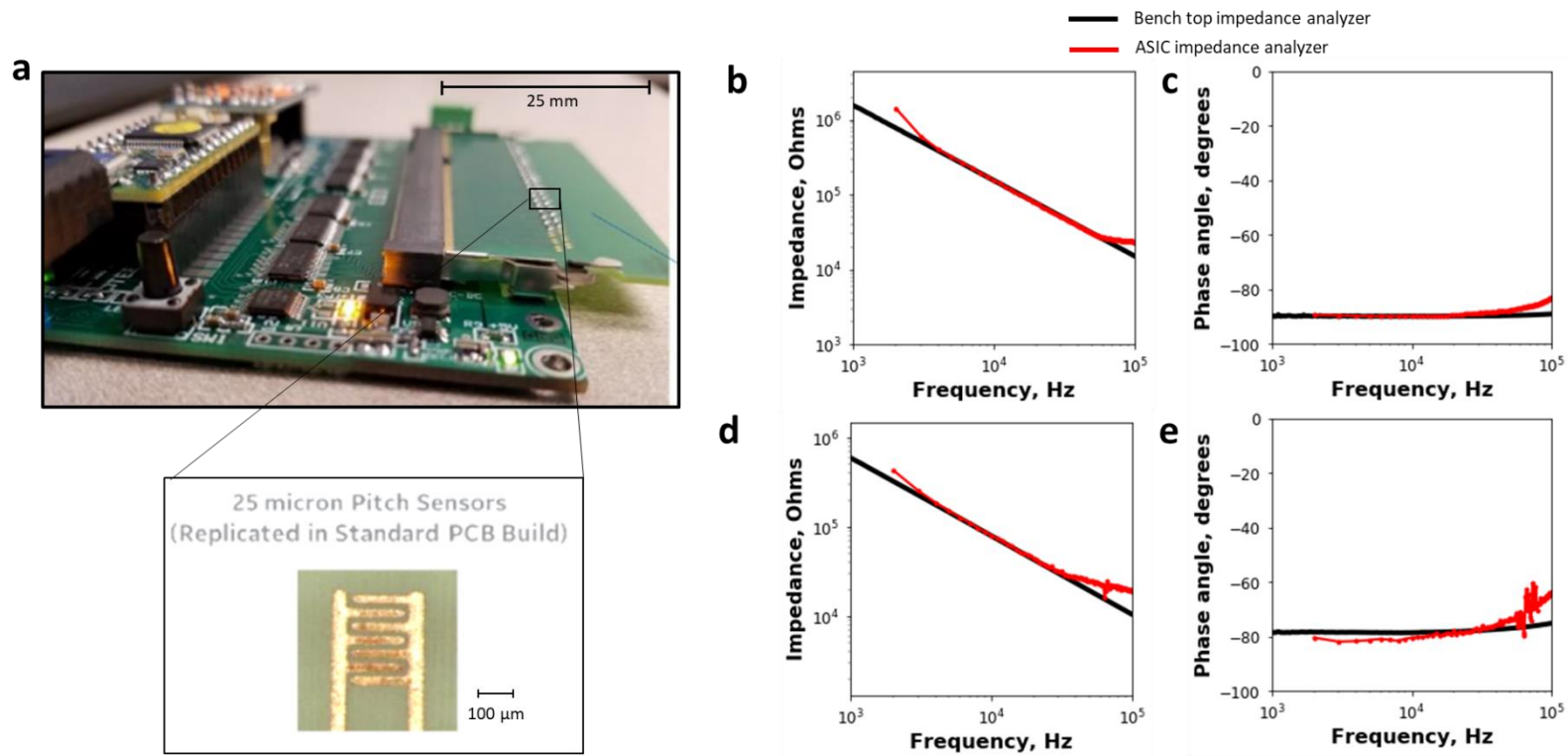


**Fig. S1** Hand-held multiplexed impedance sensor system. (a) Side view showing a prototype PCB-based nanowell array that is loaded into the DIMM socket (instead of the glass slide based nanowell array). (b-e) Benchmark data showing the impedance measured by the ASIC impedance analyzer on the multiplexed impedance sensor system matched the impedance measured on a bench top impedance analyzer (Keysight E49990A). Panels b and c show impedance data measured on a reference circuit (this data is repeated from Fig. 1 in the main text). Panels d and e show impedance data measured on a nanowell array loaded with broth only.

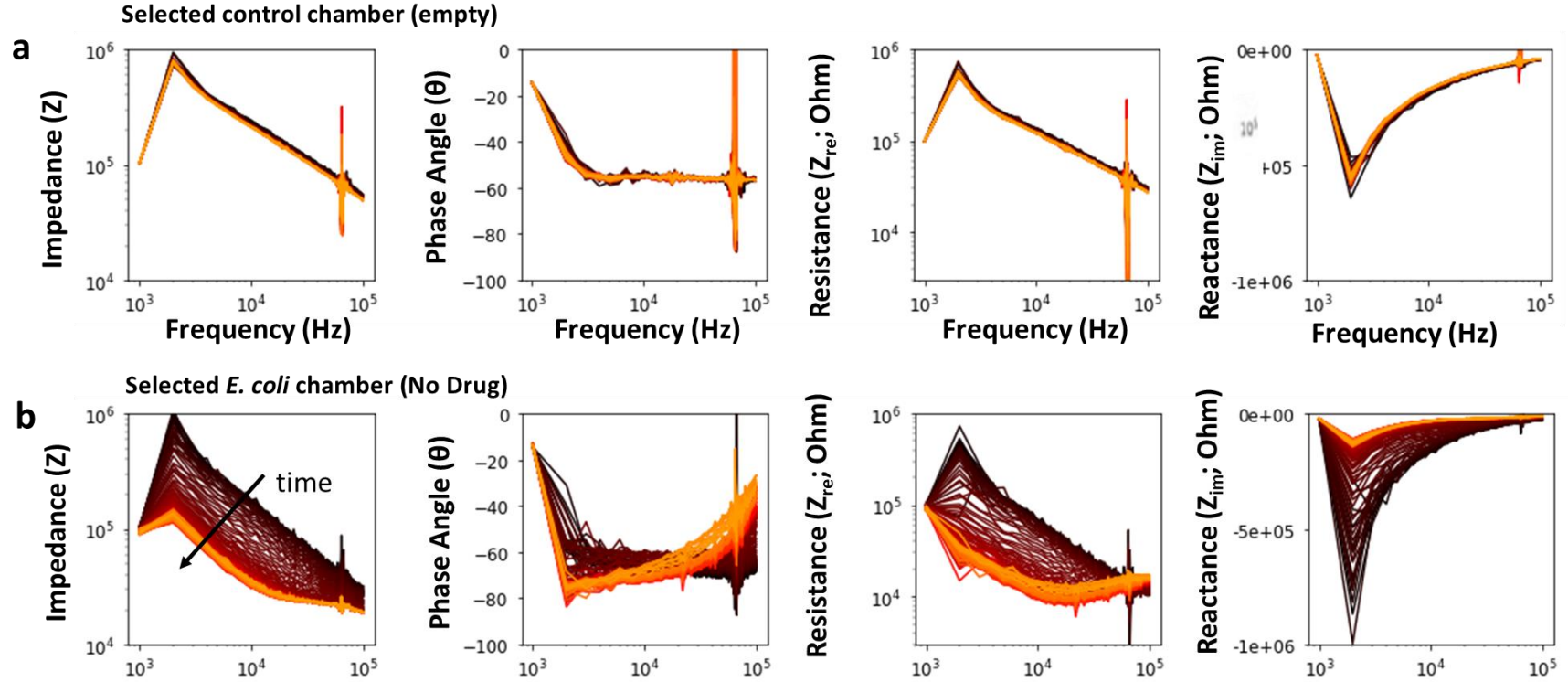


**Fig. S2:** Impedance spectra measured on the hand-held multiplexed impedance sensor for a (a) nanowell from a control sample (i.e., broth only, no bacteria) and a nanowell that contains *E. coli*.

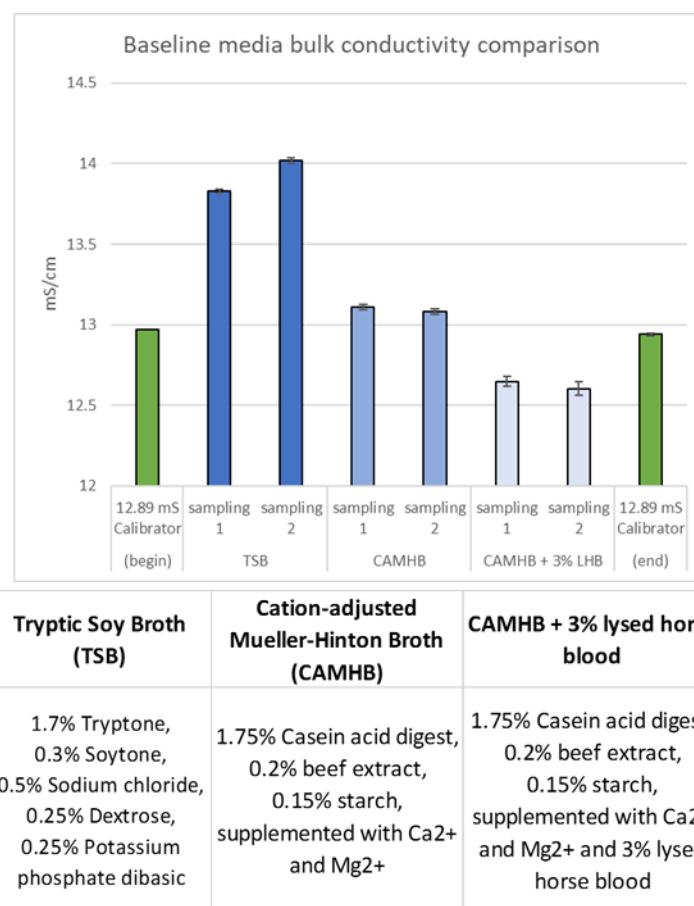


**Fig. S3** Intrinsic bulk conductivity differences among typical microbial mediums used for AST. Conductivity was measured using a Mettler-Toledo Seven Compact meter that was calibrated against 12.89 mS Standard Conductivity Calibration Solution. Two 1-mL aliquots of medium were sampled and analyzed, with careful washing of the Mettler-Toledo conductivity probe between each measurement. A final measurement against 12.89 mS Calibration Solution is shown to demonstrate effective probe washing. The contents of each growth medium are listed and support a potential relationship between salt content and bulk conductivity.

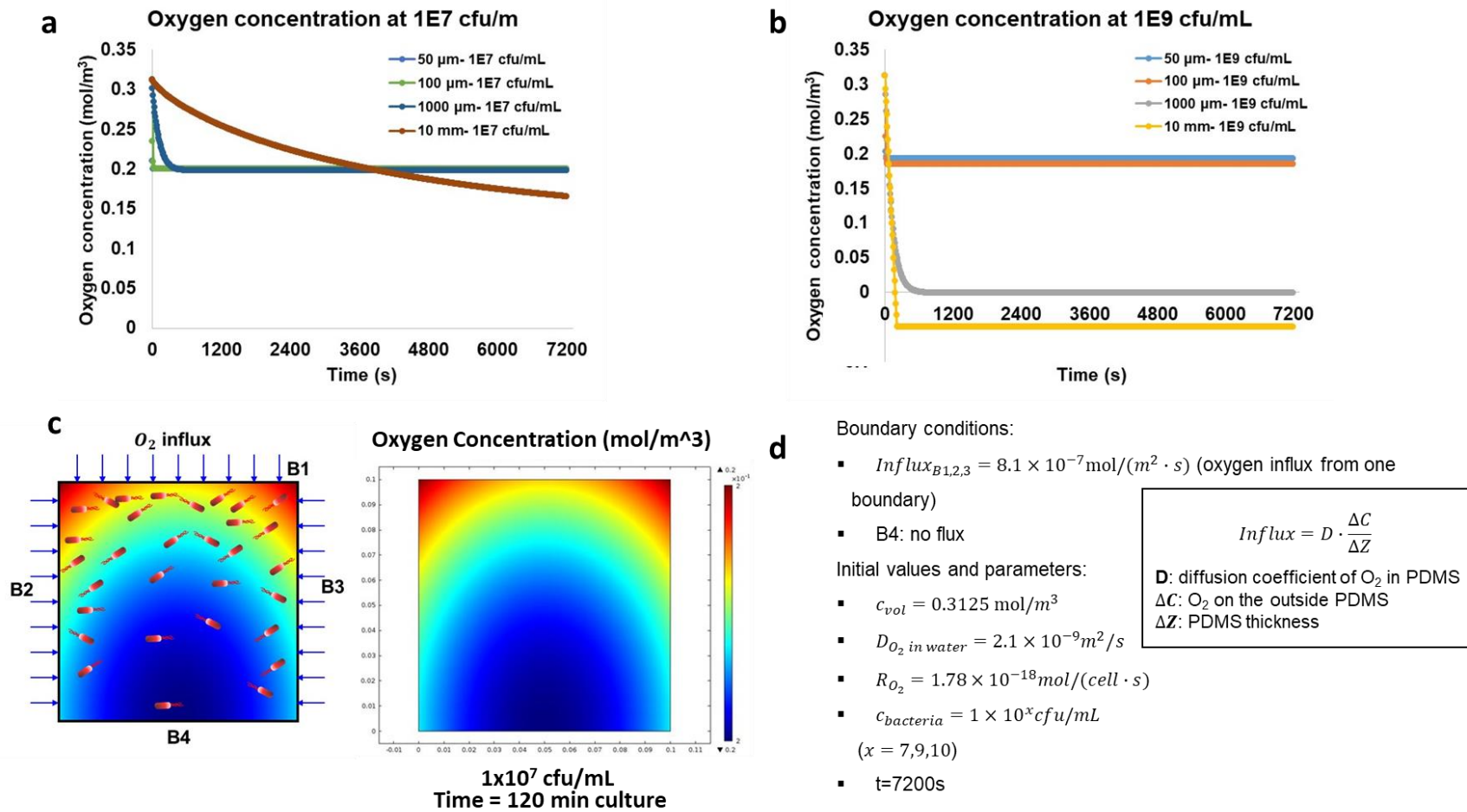
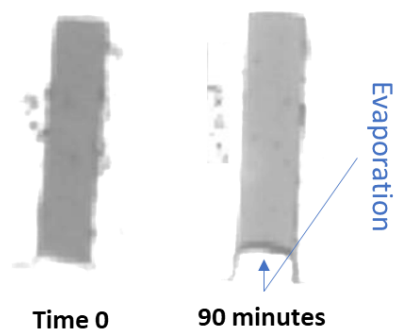
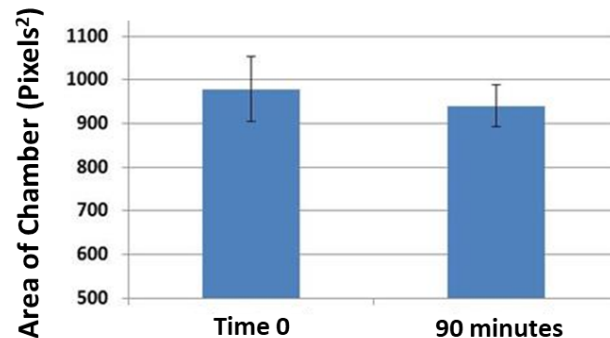


**Fig. S4** Numerical simulation to estimate the oxygen concentration in the microfluidic device. (a-b) Depletion of oxygen in microfluidic chambers at a bacterial load of (a)  $10^7$  and (b)  $10^9$  cfu/mL. (c) Schematic of the 2D model of nanoliter chambers for single bacterial growth. Blue arrows indicate oxygen influx from the boundaries (B1-B3). (d) Boundary conditions and parameters of the simulation. B1-B3 have the same oxygen influx. B4 has zero oxygen influx. The numerical calculation was performed in Comsol.

**a Measuring Evaporation Rates**

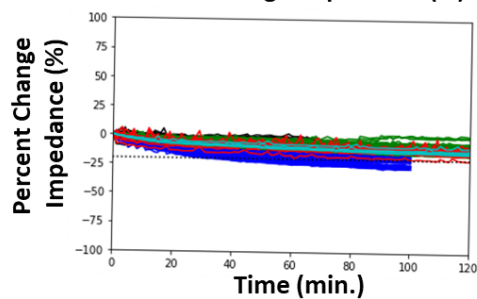
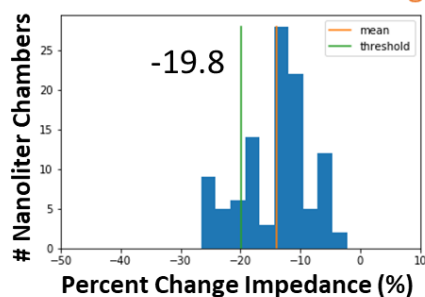


**b**

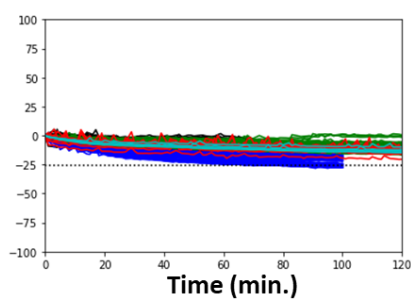
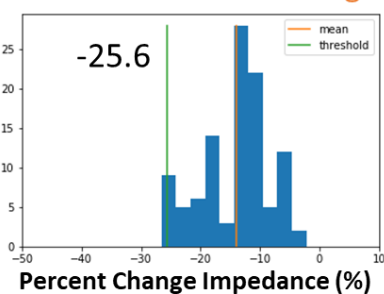


**c**

Threshold = mean - 1\*sigma



Threshold = mean - 2\*sigma



Threshold = mean - 3\*sigma

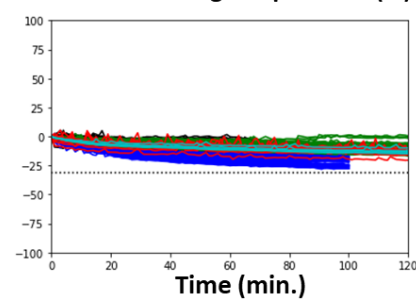
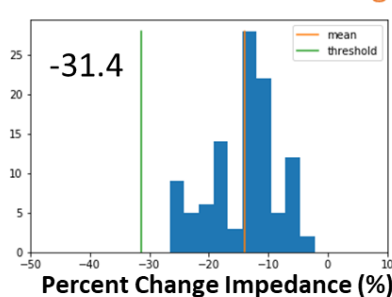


**Fig. S5** Evaporation observed in a nanowell (a) initially at the start of experiment and (b) after 90 minutes. The evaporation rate limits the total experimental duration and needs to be minimized. (c) The impedance from control samples was used to determine the positive detection threshold. For experiments reported in the main text, we used a 3 sigma detection threshold, which classifies a nanowell as positive when the impedance change is less than -31.4%.

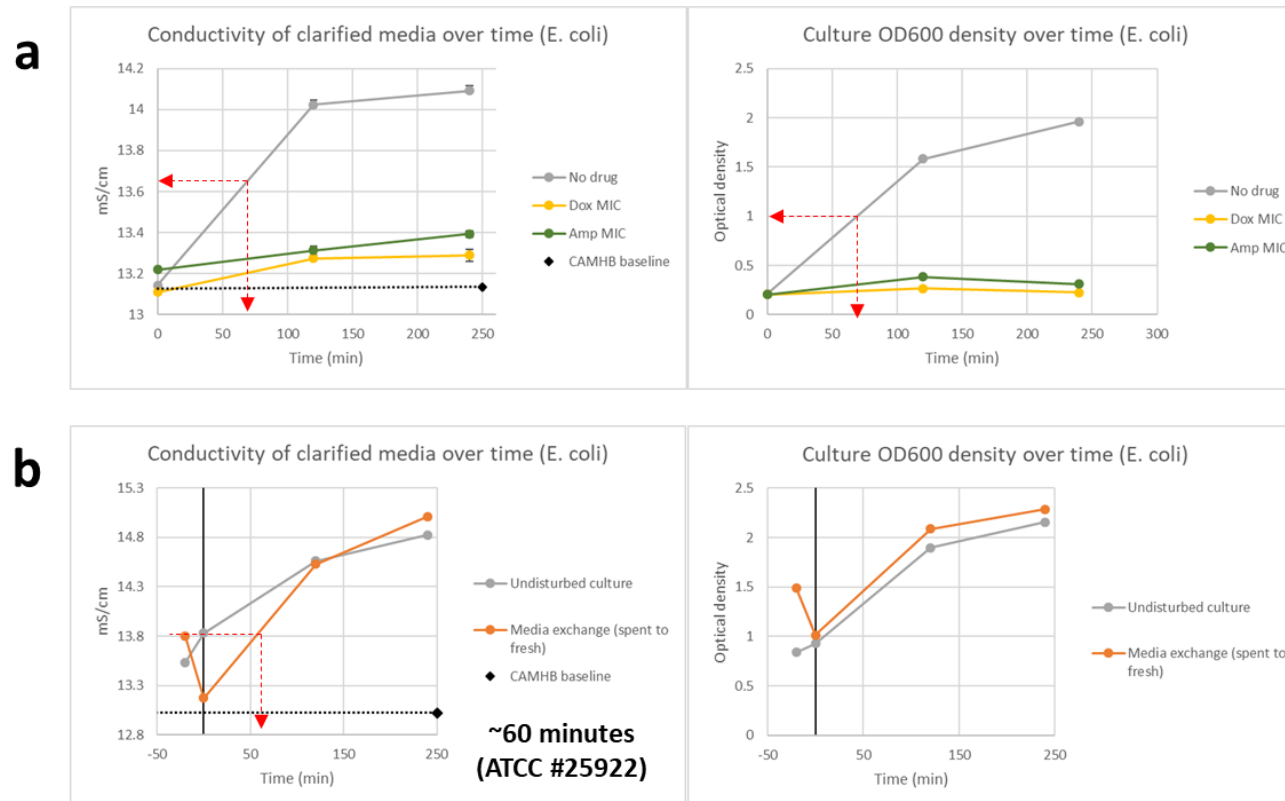


**Fig. S6 (a)** Kinetic relationship between media conductivity and culture density during AST relative to no-drug control. Experiments were performed with *E. coli* (ATCC 25922) as described in the Materials and Methods for bulk-scale culture conductivity. Culture turbidity was monitored by  $A_{600}$  optical density, after which 1mL aliquots were clarified by centrifugation and media conductivity was measured on a Mettler-Toledo Seven Compact meter. Significant differences in bulk conductivity and MIC are increasingly observed as the growth of the no-drug control approaches and exceeds  $OD_{600} \sim 1.0$  (or  $\sim 1$  cell/picoliter). After obtaining 1  $OD_{600}$  ( $\sim 1$  cell/pL), no-drug control measurements are of sufficient dynamic range and persistence to interpret MIC from conductivity data (using either doxycycline or ampicillin). Culture inoculums at Time 0 in these experiments were approximately 0.2  $OD_{600}$  (or  $\sim 2 \times 10^8$ /mL) and achieved 1  $OD_{600}$  ( $\sim 1$  cell/pL) within an hour of culture time, as indicated by the red arrows. **(b)** Recovery of bulk conductivity in fresh media (after spent media exchange) confirms time-to-detection for achieving  $\sim 1$  cell/picoliter in no-drug controls. Experiments were performed with *E. coli* as described in the Materials and Methods for bulk-scale culture conductivity. Late log-growth cultures ( $\sim 1$   $OD_{600}$ ) were centrifuged and exchanged into fresh media, and conductivity was monitored after media-exchange relative to undisturbed culture controls. The recovery of initial conductivity for cells shifted into fresh media occurs after  $\sim 60$  minutes of culture time, consistent with Panel A. By extrapolation, this data informs that an hour of culture time should be sufficient for growth detection of *E. coli* in nanoliter culture arrays.

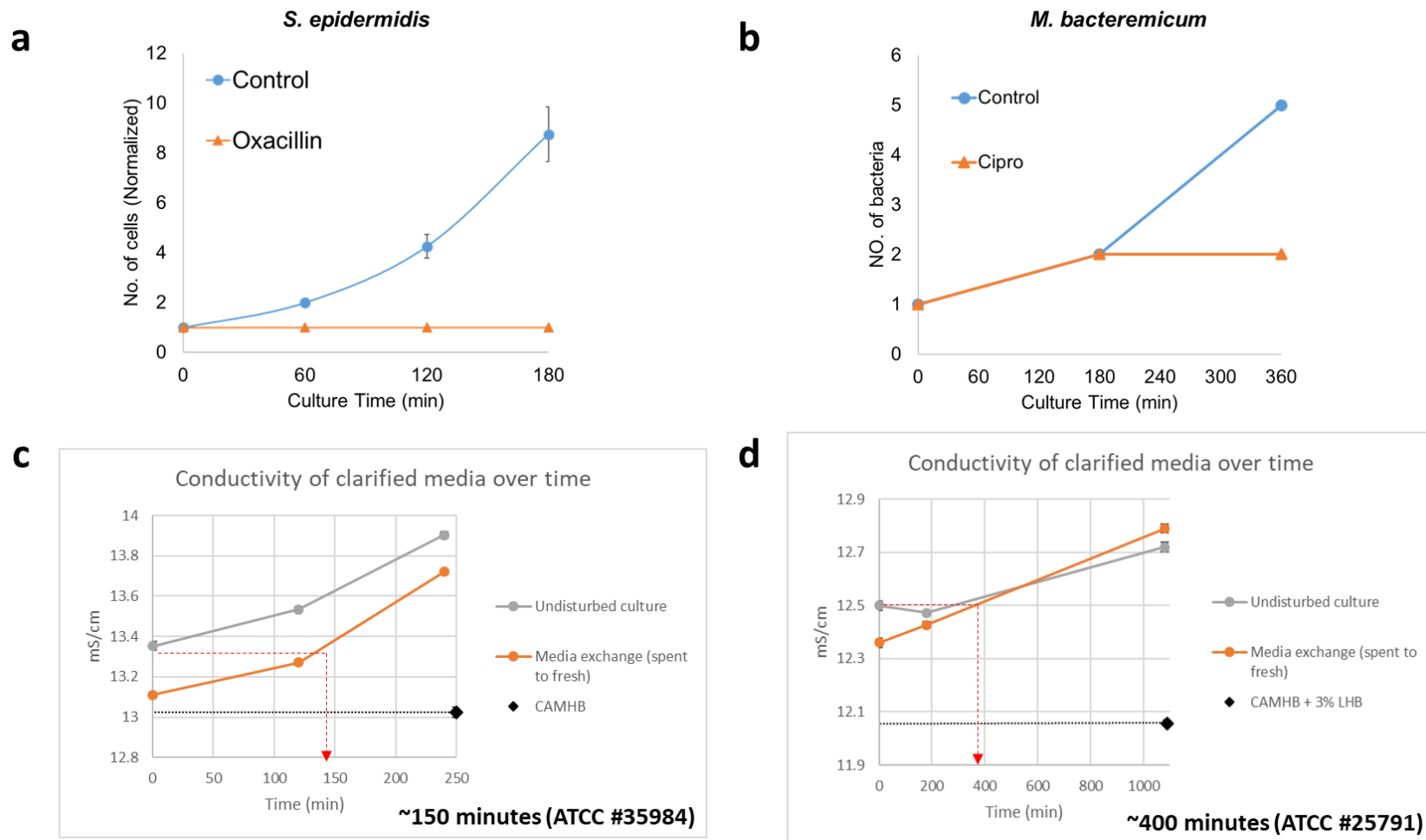


**Fig. S7** (a, b) Comparison of nanoliter culture array data for additional microbial strains using optical monitoring and cell counting. Cultures of *S. epidermidis* (ATCC 35984) and *M. bacteremicum* (ATCC 25791) were loaded into nanoliter culture arrays for optical inspection and digital counting per chamber. Antibiotics were included in duplicate samples to demonstrate AST. (c, d) Recovery of conductivity in fresh media after spend media exchange of (c) *S. epidermidis* (MRSE) or (d) *M. bacteremicum* cultures. Experiments were performed similarly to Fig. S8. The recovery of initial conductivity for MRSE (after exchange into fresh medium) was observed after ~150 minutes of culture time (panel a), whereas for the fastidious *M. bacteremicum* strain (which requires extra medium supplementation with 3% LHB) recovery of conductivity was observed after ~400 minutes of culture time (panel b). By extrapolation, this data informs that much longer culture times (minimum 2.5 hrs) would be required for robust growth detection of these strains in nanoliter culture arrays.

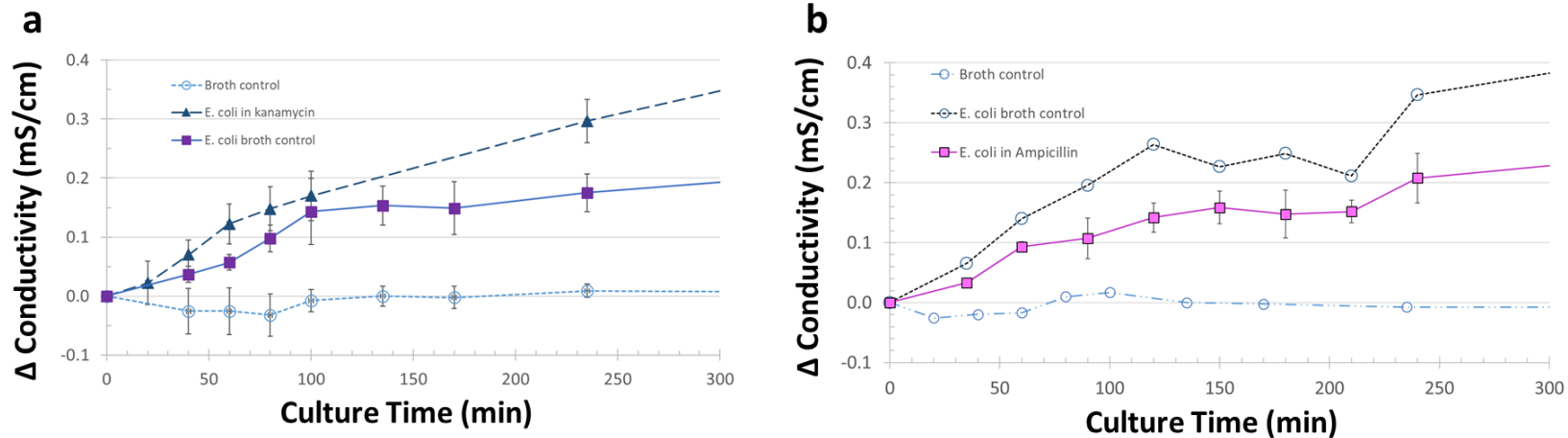


**Fig. S8** The model system from Fig. 3 in the main text was used here to test effect of antimicrobials on bacteria growth. Media conductivity increase is detectably suppressed when bacterial growth is inhibited by antimicrobial drugs. *E. coli* (ATCC 25922) was grown to mid-log phase in rich medium (Tryptic Soy broth) and inoculated into 20 ml fresh medium to a density of 108 cells/ml in presence or absence of (a) Kanamycin at 50 ug/ml, or (b) Ampicillin at 40 ug/ml. Each growth condition was replicated in triplicate and measurements made in parallel. Aliquots of 1 ml were withdrawn at indicated times, immediately chilled on ice, and clarified by centrifugation at 12,000 x g for 5 min at 5°C. The cell-free media supernatant was then flash-frozen at -80°C. Conductivity of the media samples was then measured on a Mettler-Toledo Seven Compact meter.

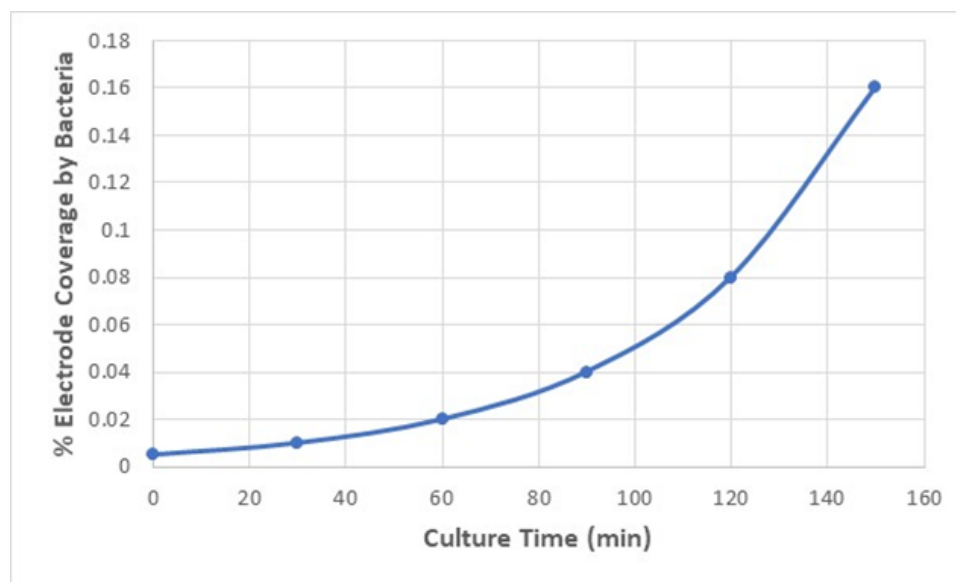


**Fig. S9** An estimation of the percent coverage of the interdigitated electrode pair during growth and doubling of a single bacterium within a nanowell. Assumptions: one *E. coli* =  $2 \mu\text{m}^2$ , and the surface area of each electrode pair =  $40,000 \mu\text{m}^2$ ). During the two hours of culture reported herein, the maximal electrode coverage by bacteria does not surpass 0.1% of the electrode surface area, which is below the cell and/or particle coverage needed to contribute to impedance-based detection schemes<sup>1-4</sup>. Taken together with Fig. 2, Fig. 6b, and Fig. S10, this suggests the accumulation of metabolites is likely the primary mechanism determining the impedance in the nanowell during growth (and not the physical presence of bacteria on the electrodes).

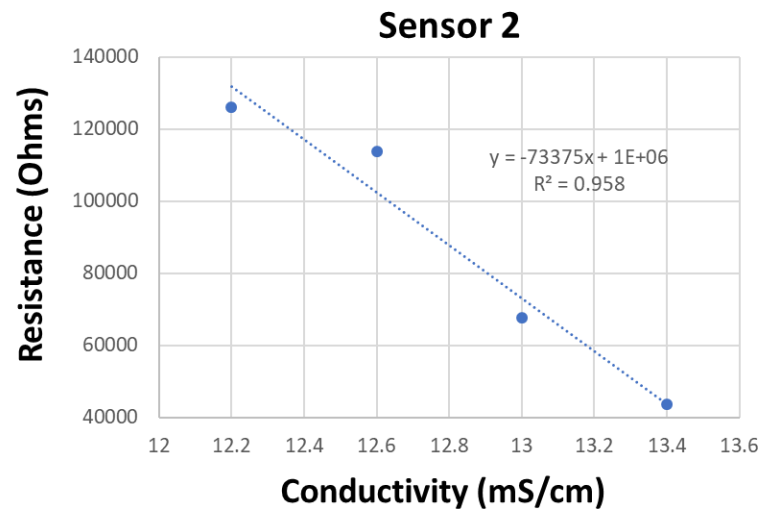
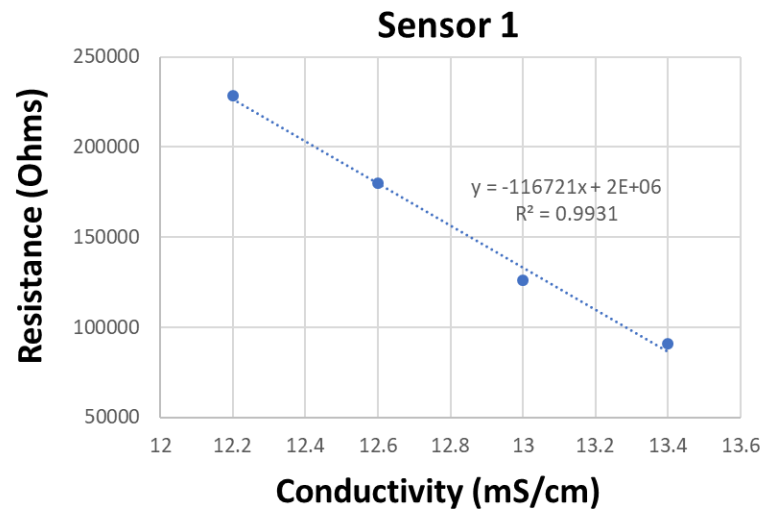


**Fig. S10** Resistance measured when serial dilutions of conductivity standards ranging from 12.2 to 13.4 mS/cm were loaded directly into the nanowell/sensor chambers (this range of conductivities is consistent with the range of conductivities determined in Fig. 2 to be associated with metabolite specific changes in the growth broth, after centrifuging out any bacteria). The change in resistance associated with the increase in conductivity of the solution within each electrode chamber is consistent with that associated with single bacterium growth.

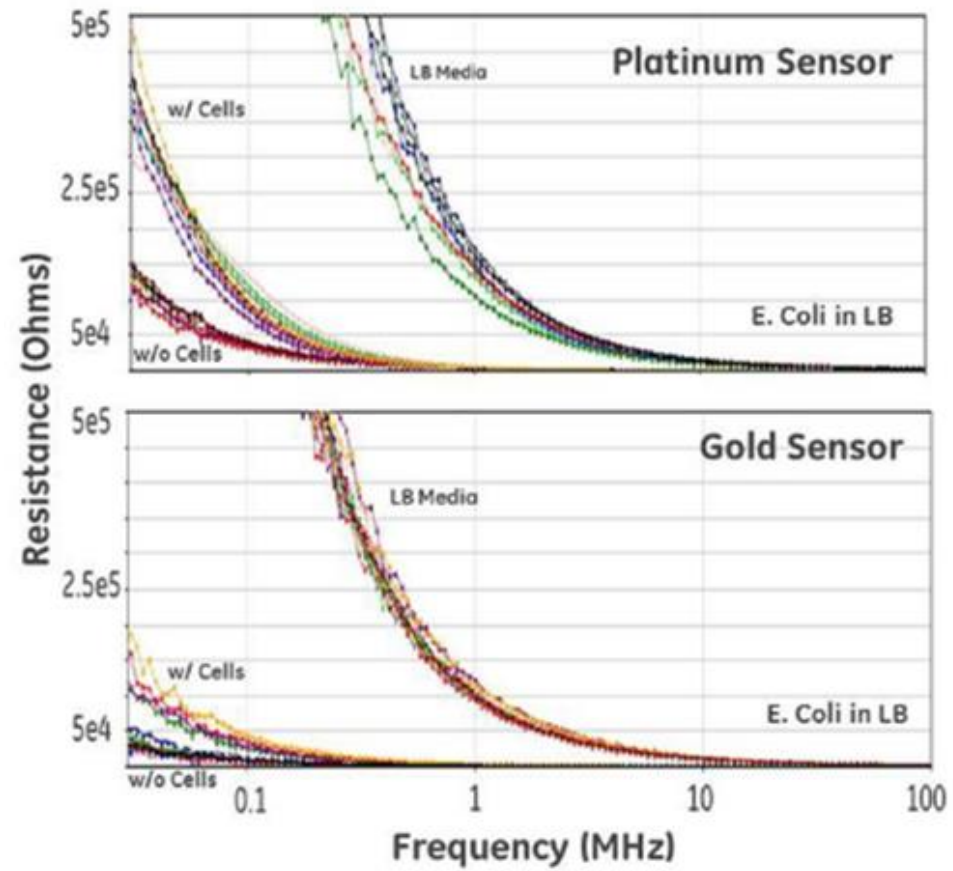


**Fig. S11** Example data showing comparison of impedance data in a gold (10  $\mu\text{m}$  electrode spacing) and platinum (10  $\mu\text{m}$  electrode spacing) interdigitated electrode sensor. Three sets of nanowells were filled with either growth broth alone before bacteria growth (i.e. LB media; lysogeny broth), broth after 2 hours of bacterial growth (w/ cells), or broth after 2 hours of bacterial growth after removal of cells via centrifugation (w/o cells).

## References

1. S. Brosel-Oliu, N. Abramova, N. Uria and A. Bratov, *Analytica Chimica Acta*, 2019, **1088**, 1–19.
2. N. Courniot, D. Flandre, L. A. Francis and A. Afzalian, *Procedia Engineering*, 2012, **47**, 188–191.
3. S. Kim, G. Yu, T. Kim, K. Shin and J. Yoon, *Electrochimica Acta*, 2012, **82**, 126–131.
4. L. Yang, Y. Li and G. F. Erf, *Anal. Chem.*, 2004, **76**, 1107–1113.